

# Conditional Knockdown of Tubedown-1 in Endothelial Cells Leads to Neovascular Retinopathy

Dana S. Wall,<sup>1</sup> Robert L. Gendron,<sup>1</sup> William V. Good,<sup>2</sup> Ewa Miskiewicz,<sup>1</sup> Mandy Woodland,<sup>1</sup> Karina Leblanc,<sup>1</sup> and H el ene Paradis<sup>1</sup>

**PURPOSE.** Identification of novel proteins involved in retinal neovascularization may facilitate new and more effective molecular-based treatments for proliferative retinopathy. Tubedown-1 (Tbdn-1) is a novel protein that shows homology to the yeast acetyltransferase subunit NAT1 and copurifies with an acetyltransferase activity. Tbdn-1 is expressed in normal retinal endothelium but is specifically suppressed in retinal endothelial cells from patients with proliferative diabetic retinopathy. The purpose of this study was to investigate the importance of Tbdn-1 expression in retinal blood vessels *in vivo*.

**METHODS.** A bitransgenic mouse model that enables conditional knockdown of Tbdn-1 specifically in endothelial cells was produced and studied using molecular, histologic, and immunohistochemical techniques and morphometric analysis.

**RESULTS.** Tbdn-1-suppressed mice exhibited retinal and choroidal neovascularization with intra- and preretinal fibrovascular lesions similar to human proliferative retinopathies. Retinal lesions observed in Tbdn-1-suppressed mice increased in severity with prolonged suppression of Tbdn-1. In comparison to normal retina, the retinal lesions displayed alterations in the basement membrane of blood vessels and in the distribution of glial and myofibroblastic cells. Moreover, the pathologic consequences of Tbdn-1 knockdown in endothelium were restricted to the retina and the choroid.

**CONCLUSIONS.** These results indicate that the maintenance of Tbdn-1 expression is important for retinal blood vessel homeostasis and for controlling retinal neovascularization in adults. Restoration of Tbdn-1 protein expression and/or activity may provide a novel approach for treating proliferative retinopathies. (*Invest Ophthalmol Vis Sci.* 2004;45:3704-3712) DOI:10.1167/iovs.03-1410

From the <sup>1</sup>Division of Basic Medical Sciences, Department of Medicine, Memorial University of Newfoundland, St. John's, Newfoundland, Canada; and the <sup>2</sup>Smith Kettlewell Eye Research Institute, San Francisco, California.

Supported by Canadian Institutes of Health Research Operating Grants, a Foundation Fighting Blindness-Canada Operating Grant, National Eye Institute Grant EY12827, and Children's Oncology Group Chairman's Award NIH U10CA13539 (RLG, HP); National Eye Institute Grants EY00384-05, EY12472-02 (WVG); and a Studentship from the Office of Graduate Studies, Memorial University of Newfoundland (DSW).

Submitted for publication December 30, 2003; revised June 15, 2004; accepted June 25, 2004.

Disclosure: **D.S. Wall**, None; **R.L. Gendron**, None; **W.V. Good**, None; **E. Miskiewicz**, None; **M. Woodland**, None; **K. Leblanc**, None; **H. Paradis**, None

The publication costs of this article were defrayed in part by page charge payment. This article must therefore be marked "advertisement" in accordance with 18 U.S.C. §1734 solely to indicate this fact.

Corresponding author: Robert L. Gendron, Division of Basic Medical Sciences, Department of Medicine, Memorial University of Newfoundland, St. John's, NL, A1B 3V6, Canada; rgendron@mun.ca.

In blinding ocular diseases such as proliferative diabetic retinopathy (PDR) and retinopathy of prematurity (ROP), initial retinal ischemia progresses to a proliferative stage that involves both neovascularization and fibrosis of the retina and results in the formation of preretinal membranes.<sup>1-8</sup> A significant cause of blindness associated with both PDR and ROP results from retinal detachment caused by membranous traction.<sup>1-8</sup> Laser photocoagulation of avascular regions of the retina reduces blindness in patients with neovascular retinopathies.<sup>1-8</sup> However, this treatment is ablative and may not prevent the sight-impairing complications associated with the retinopathy.<sup>1-8</sup> Elucidating the molecular processes of proliferative retinal disease and designing therapies to target molecular abnormalities may offer a means to replace laser surgery and prevent associated complications.

The molecular events leading to the angiogenic process in PDR and ROP are believed to be mediated by increased expression of proangiogenic growth factors (vascular endothelial growth factor [VEGF], basic fibroblast growth factor [bFGF], and insulin-like growth factor [IGF-1]).<sup>5,9-11</sup> Integrins, extracellular matrix (ECM) components, and glial cells also contribute to pathologic neovascularization in PDR.<sup>5,10-13</sup> Increased production of VEGF in the retina is probably the determining factor in the proliferative neovascularization that leads to pathologic sequelae in later stages of diabetic retinopathy (DR).<sup>9,10,14,15</sup> Treatments specifically targeting either VEGF and its receptors or specific integrins have been effective in reducing but not abolishing retinal neovascularization in animal models.<sup>9</sup> Moreover, these treatments do not completely or consistently rescue preexisting disease. Because a range of angiogenic factors in the microenvironment probably promote retinal blood vessel proliferation, the targeting of one type of factor for antiangiogenic therapy may not completely counter the neovascularization in DR. The characterization of common regulators acting in diverse angiogenic pathways is key to identifying targets that could have a more global effect on controlling retinal neovascularization.

Tubedown-1 (Tbdn-1) is a mammalian homologue of the yeast acetyltransferase subunit NAT1.<sup>16</sup> Tbdn-1 expression is regulated during development and becomes restricted to normal ocular endothelial cells, atrial endocardium, blood vessels of regressing ovarian follicles, and bone marrow capillaries in adults.<sup>16,17</sup> We have found that Tbdn-1 expression is suppressed in retinal blood vessels in patients with PDR.<sup>17</sup> Both *in vitro* experiments and *in vivo* observations have suggested that Tbdn-1 suppression in retinal endothelial cells leads to increased angiogenesis.<sup>16-18</sup> Collectively, these data have led us to hypothesize that Tbdn-1 functions to suppress retinal neovascularization *in vivo*. To directly examine whether Tbdn-1 is an important regulator of retinal neovascularization *in vivo*, we have generated a binary antisense *TBDN-1* (*ASTBDN-1*) transgenic mouse model driven by *TIE2* panendothelial promoter to enable conditional knockdown of Tbdn-1 expression in endothelial cells. We present *in vivo* evidence for the requirement of Tbdn-1 expression for the maintenance of normal adult retinal vascular homeostasis.

## METHODS

### Endothelium-Specific Conditional Knockdown of Tbdn-1 in a Bitransgenic Mouse Model

To facilitate conditional knockdown of Tbdn-1 in endothelial cells in mice, we derived two different lines of transgenic mice. For the construction of the first line, the *Bam*HI/*Pvu*II fragment from pcDNA3.1/*Zeo*-*ASTBDN-1*<sup>18</sup> containing the antisense cDNA fragment sequence 1-1413 of *TBDN-1* was inserted into the pTRE vector (BD-Clonotech, Palo Alto, CA) at the *Bam*HI and *Pvu*II sites. This antisense *TBDN-1* fragment 1413-1 does not produce aberrant proteins that could confer toxic and nonspecific effects. The resultant construct pTRE/*ASTBDN-1* was digested with *Aat*II and *Pvu*II. The fragment containing the TRE promoter followed by *ASTBDN-1* (*TRE/ASTBDN-1*) was used to create FVB transgenic mouse lines (Transgenic Core Facility, Children's Hospital Research Foundation, Cincinnati, OH).

Construction of the second line of transgenic mice was as follows: A DNA fragment encompassing coding sequences for *rtTA* followed by the SV40 polyA site were amplified by PCR from the pTet-On vector (BD-Clonotech) using the following primers: 5'-CGGCCCGAATTA-ATATGGCTAGATTA-3' and 5'-TCCATTTAGCGGCCGAGCTCCT-GAA-3'. The purified amplicon was digested with *Hind*III and *Not*I and inserted into the pHSDKXXK construct<sup>19</sup> previously digested with *Hind*III and *Not*I, removing the HH (*Hind*III to *Hind*III) portion of the promoter and the coding sequences for *LacZ* (SDK). The resultant construct, pHrtTAXK, was digested with *Apa*I and ligated with the HH portion of the promoter previously amplified from the pHSDKXXK construct (using primers 5'-TGGTACCGGGCCCCCT-3' and 5'-TCATCGCGGGCCCTGGTGGCCCT-3'), and digested with *Apa*I. Orientation of the *TIE2* promoter in the construct was verified to be as previously described for endothelial specificity.<sup>19</sup> The resultant construct pHHrtTAXK was digested with *Kpn*I and the fragment harboring the *TIE2* promoter, *rtTA* coding sequence, SV40 polyA site, and *TIE2* enhancer (*TIE2/rtTA/Enb*) was used to create FVB transgenic mouse lines (Transgenic Core Facility at Children's Hospital Research Foundation).

Genotyping was performed by Southern blot analysis using either a probe encompassing the *TRE* promoter for the *TRE/ASTBDN-1* transgenic lines or a probe encompassing the coding sequence for *rtTA* for the *TIE2/rtTA/Enb* lines. Lines positive for HHrtTAXK transgene integration were further tested for *rtTA* protein expression by Western blot analysis<sup>18</sup> of lysates of tail specimens and by immunohistochemistry of the vasculature, with an affinity-purified rabbit polyclonal antibody that recognizes the VP-16 sequence present in the *rtTA* protein (BD-Clonotech). FVB transgenic lines were backcrossed into the C57BL/6 background. Bitransgenic *TIE2/rtTA/Enb-TRE/ASTBDN-1* mice were derived by mating four different *TRE/ASTBDN-1*-positive lines to five different *TIE2/rtTA/Enb*-positive lines.

For conditional knockdown of Tbdn-1, induction with doxycycline (Dox) was performed by feeding adult animals with commercially prepared mouse chow containing Dox (600 mg/kg; Bio-Serv, Frenchtown, NJ). Dox-fed mice were killed at various time points and analyzed grossly, histologically, and immunohistochemically for disease. The care and use of animals in this study followed the guidelines set forward by the Canadian Council on Animal Care and were approved by the Institutional Animal Care Committee of Memorial University of Newfoundland. All experiments involving animals adhered to the ARVO Statement for the Use of Animals in Ophthalmic and Vision Research.

### Mouse Anti-Tbdn-1 Serum and Western Blot Analysis for Retinal Tbdn-1

To generate a mouse anti-Tbdn-1 serum (MS.C1-20TD), mice were immunized with a peptide corresponding to the amino acid sequence 10-20 of mouse Tbdn-1<sup>16</sup> coupled to cBSA (Pierce, Rockford, IL). The specificity of the mouse anti-Tbdn-1 antiserum, was validated by confirming that recombinant Tbdn-1 protein was immunoprecipitated by

MS.C10-20TD antiserum. Briefly, in vitro translation of Tbdn-1 was performed with a translation/transcription system (TNT T7 Quick Coupled Transcription/Translation System; Promega, Madison, WI), using [<sup>35</sup>S]-methionine/cysteine and the pcDNA3.1-*TBDN-1* construct.<sup>16</sup> Analysis of immunoprecipitations of in vitro-translated <sup>35</sup>S-labeled Tbdn-1 with the mouse anti-Tbdn-1 serum MS.C10-20TD was as has been described.<sup>18</sup> Retinas from Dox-induced *TIE2/rtTA/Enb-TRE/ASTBDN-1* and control mice were isolated from surrounding sclera, vitreous, and other ocular tissues. Western blot analysis for Tbdn-1 expression in retinal tissues from Dox-induced *TIE2/rtTA/Enb-TRE/ASTBDN-1* and control mice was performed with chicken anti-Tbdn-1 AB1272 antibody, as has been described.<sup>18</sup>

### Histology and Immunohistochemistry of Tbdn-1-Suppressed Mice

Mouse tissues were fixed in 4% paraformaldehyde, embedded in paraffin or methacrylate resin, and processed for histology and immunohistochemistry, as previously described.<sup>18,20</sup> Sections were stained with hematoxylin and eosin (H&E), toluidine blue, or different antibodies. Antibodies used for immunohistochemistry included chicken anti-Tbdn-1 Ab1272 antibody,<sup>16</sup> mouse anti-Tbdn-1 serum MS.C10-20TD, rabbit anti-VP-16 (BD-Clonotech), rabbit anti-von Willebrand factor (vWF; Dako, Carpinteria, CA), rabbit anti-laminin (Dako), mouse anti-glial fibrillary acidic protein (GFAP), and mouse anti- $\alpha$  smooth muscle actin ( $\alpha$ -SMA; Sigma-Aldrich). Mouse anti-basement membrane heparan sulfate proteoglycan (HSPG) antibodies C17<sup>21</sup> and -33<sup>22</sup> were obtained from Developmental Studies Hybridoma Bank (University of Iowa, Iowa City, IA). Immunohistochemistry reactions were developed with a species-appropriate secondary antibody (Promega) conjugated to alkaline phosphatase or horseradish peroxidase. The sections were counterstained with methyl green and mounted (Permount; Fisher Scientific, Pittsburgh, PA). Sections destined for peroxidase development were previously incubated in 0.3% hydrogen peroxide for 10 minutes to block endogenous peroxidase activity. Before incubation with anti-laminin, tissues were digested with 0.1% trypsin at 35°C for 20 minutes. Mouse antibodies were applied after a 30-minute incubation in rabbit anti-mouse blocking preparation.

### Blood Vessel Counts and Morphometric Analysis

Tissue sections of retina, choroid, liver, kidney, brain, and testes were examined under a light microscope using a CCD camera (QImaging; Burnaby, British Columbia, Canada) and digital imaging software (Openlab; Improvision, Lexington, MA) at 250 $\times$  magnification (liver, brain, kidney, and testes) or 400 $\times$  magnification (retina and choroid) after H&E staining and/or immunostaining with laminin or vWF-specific antibodies, as described earlier. Blood vessel densities were observed in detail in liver parenchyma, kidney cortex, testis interstices, cerebral cortex, areas along surfaces of brain ventricles, and cerebellum. Areas along surfaces of brain ventricles were sampled, because this aspect of the brain most closely resembles inner layers of the retina. For retinal and choroidal tissue analysis, digital photographs were taken in areas of the central retina where disease is mostly observed. The blood vessels in the different retinal layers and choroid were counted per square micrometer of each layer. For retina and choroid, 25 specimens (mice) consisting of 14 control and 11 Dox-induced bitransgenic mice (three 2-week Dox-induced, five 6 week Dox-induced, and three 12-week Dox-induced) were analyzed. Liver parenchyma and kidney cortex blood vessels were counted in 10 random nonoverlapping areas (35,200  $\mu$ m<sup>2</sup>/area) within two independent sections for each treatment with two specimens per treatment. Tissue thickness in the inner and outer retinal layers and choroid was measured using digital calipers, and blood vessel counts were performed by counting either laminin or H&E-stained blood vessels on digital micrographs (QImaging CCD camera; and Openlab software; Improvision).

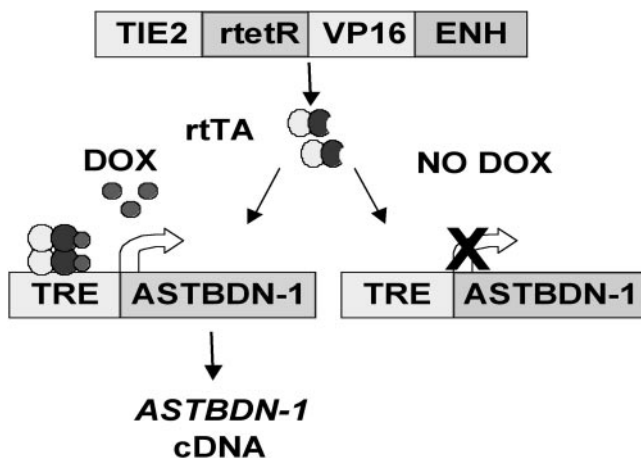


**FIGURE 1.** Conditional knockdown of Tbdn-1 in endothelial cells using a bitransgenic model. The *TIE2* endothelium-specific promoter regulates the expression of the rtTA protein in endothelium. In the presence of Dox, rtTA binds and activates the tetracycline response element (*TRE*) promoter, which directs the expression of an antisense *TBDN-1* cDNA (*ASTBDN-1*). In the absence of Dox, rtTA does not bind the *TRE* promoter, and the *ASTBDN-1* is not expressed.

## RESULTS

### Conditional Knockdown of Tbdn-1 in Endothelium of *TIE2/rtTA/Enb-TRE/ASTBDN-1* Bitransgenic Mice

To explore the role of Tbdn-1 in endothelium *in vivo*, we generated a binary antisense *TBDN-1* (*ASTBDN-1*) transgenic mouse model (*TRE/ASTBDN-1* and *TIE2/rtTA/Enb*) driven by the tetracycline-responsive element (*TRE*) and the *rtTA* cDNA under the control of the *TIE2* endothelial promoter, to conditionally suppress Tbdn-1 expression after Dox treatment (Fig. 1). The *TIE2* promoter confers transgene expression in all endothelial cells, including retinal endothelium *in vivo*.<sup>19</sup> Expression of the rtTA protein in the vasculature of mouse lines identified to contain the *TIE2/rtTA/Enb* sequences was confirmed by Western blot and immunohistochemical analyses of tissues such as the endocardium and bone marrow blood vessels compared with nontransgenic control mice (Fig. 2a, 2b and not shown). Mice harboring both *TIE2/rtTA/Enb* and *TRE/ASTBDN-1* transgenes were treated with Dox and analyzed for efficacy in specifically suppressing Tbdn-1 levels in the endothelium. Dox-induced *TIE2/rtTA/Enb-TRE/ASTBDN-1* mice showed suppression of Tbdn-1 protein expression in both retinal blood vessels and bone marrow blood vessels, when compared with bitransgenic noninduced animals or single-transgene Dox-induced control animals (Figs. 2c-f and not shown).

To confirm our immunohistochemical findings that Dox-induced *TIE2/rtTA/Enb-TRE/ASTBDN-1* mice show suppression of Tbdn-1 protein expression in retinal blood vessels, Western blot analysis for Tbdn-1 was performed on isolated retinal tissues from Dox-induced *TIE2/rtTA/Enb-TRE/ASTBDN-1* and control mice. As shown in Figure 3, retinal tissue from 6-week Dox-induced *TIE2/rtTA/Enb-TRE/ASTBDN-1* mice showed a decrease in the 69-kDa Tbdn-1-specific protein band (Fig. 3, left, lane 3, and right, lane 2) compared with wild-type (Fig. 3, left, lane 1) and rtTA single transgenic (Fig. 3, left, lane 2, and right, lane 1) control animals.

To confirm that the specific knockdown of Tbdn-1 expression in double-induced transgenic mice does not result from the loss of retinal blood vessels, basal lamina of retinal blood

vessels of either noninduced or Dox-induced *TIE2/rtTA/Enb-TRE/ASTBDN-1* were stained for laminin. Laminin staining of sections adjacent to those showing Tbdn-1 suppression revealed the presence of complex vascular networks, ruling out the loss of retinal blood vessels in Dox-induced *TIE2/rtTA/Enb-TRE/ASTBDN-1* mice (Figs. 2g, 2h). Moreover, laminin staining of the basal lamina of retinal blood vessels indicates a focal increase in blood vessel density in Tbdn-1-suppressed retinas, compared with control specimens (Figs. 2g, 2h, 4a, 4b).

### Effect of Conditional Knockdown of Tbdn-1 in Endothelium

Morphologic assessment of retinas in Dox-induced *TIE2/rtTA/Enb-TRE/ASTBDN-1* mice in which Tbdn-1 was suppressed in endothelial cells ( $n = 15$ ) revealed a phenotype characterized by the formation of preretinal membranes displaying retinal neovascularization, fibrovascular growth, and retina-lens adhe-

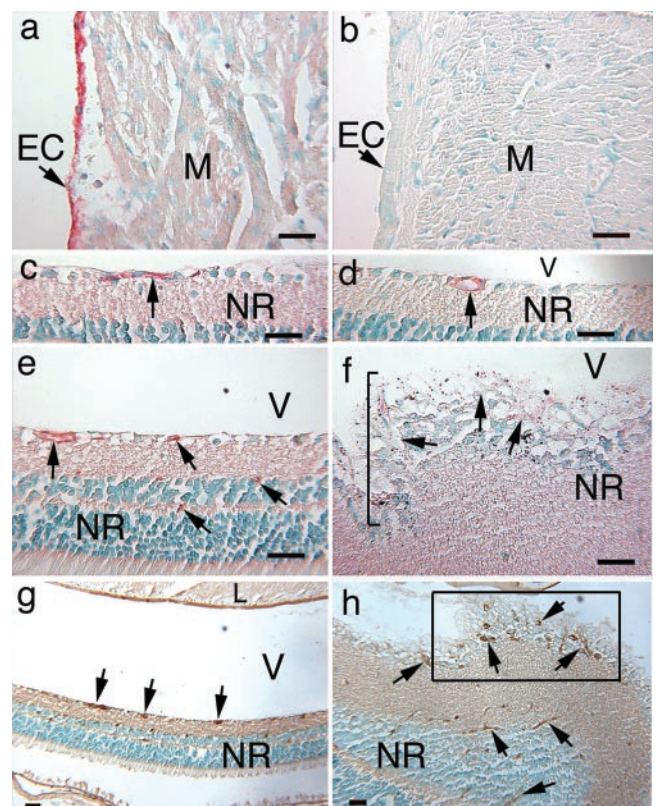


**FIGURE 2.** Conditional knockdown of Tbdn-1 in blood vessels of *TIE2/rtTA/Enb-TRE/ASTBDN-1* bitransgenic mice. (a, b) Immunohistochemical analysis of rtTA protein expression (positive red staining) in heart tissue from mice harboring the *TIE2/rtTA/Enb* construct (a) compared with nontransgenic mice (b). Arrows: endocardium (EC) and myocardium (M). (c-f) Tbdn-1 immunohistochemical analysis (red staining) of retinal vessels in sections of noninduced *TIE2/rtTA/Enb-TRE/ASTBDN-1* (c), 6-week Dox-induced *TRE/ASTBDN-1* (d), and 6-week Dox-induced *TIE2/rtTA/Enb-TRE/ASTBDN-1* (e, f) transgenics. (c-h, arrows) Retinal blood vessels; (f, bracket) a preretinal membrane. (g) Vascular network revealed by laminin staining (brown) of the basal lamina of retinal vessels of an adjacent section of the noninduced *TIE2/rtTA/Enb-TRE/ASTBDN-1* specimen shown in (e) and (h) of an adjacent section of the 6-week Dox-induced *TIE2/rtTA/Enb-TRE/ASTBDN-1* specimen shown in (f). Arrows: brown (horseradish peroxidase) laminin-positive vessels. (h, boxed area) Low-magnification view of a section adjacent to the diseased area in (f). V, vitreous; NR, neural retina; L, lens. Counterstain of all sections was methyl green. Scale bars, 25  $\mu$ m. Magnification: (a-f)  $\times 250$ ; (g, h)  $\times 100$ .

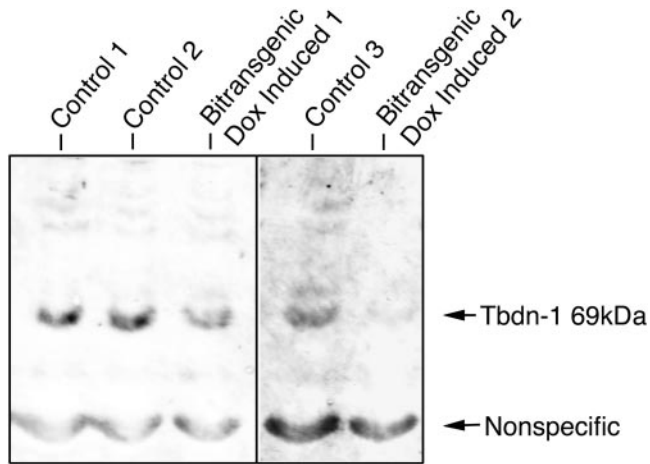


**FIGURE 3.** Conditional knockdown of Tbdn-1 in retinal tissue of *TIE2/rtTA/Enb-TRE/ASTBDN-1* bitransgenic mice. Western blot analysis for Tbdn-1 was performed on isolated retinal tissues from 6-week Dox-induced *TIE2/rtTA/Enb-TRE/ASTBDN-1* (bitransgenic [1] and [2]) and control mice (control [1], [2], and [3]). Retinal tissue from separate 6-week Dox-induced *TIE2/rtTA/Enb-TRE/ASTBDN-1* mice showed a decrease in the 69-kDa Tbdn-1-specific protein band compared with wild-type (control [1]) and *TIE2/rtTA/Enb* transgenic control animals (control [2] and [3]), respectively. The nonspecific band indicated did not vary in these samples, indicating that the knockdown of the Tbdn-1 69-kDa protein band is specific.

sions (Figs. 2c-h, 4, 5, 6, 7). Knockdown of Tbdn-1 in retinal blood vessels resulted in abnormal retinal blood vessel structures and patterns as well as an increase in numbers of retinal blood vessels and capillaries (Figs. 2h, 4b, 5c-f, 6, 7a). Retinal and vitreous tissues of Tbdn-1-suppressed mice contained a tortuous, highly branched capillary vasculature interlaced in a fibrovascular material extending beyond the vitreoretinal boarder (Figs. 2h, 4b, 5c-f, 6, 7a, 7b). Some capillaries within the retinal lesions appeared abnormally elongated and distended. In contrast, Dox-induced *TRE/ASTBDN-1* mice, Dox-induced *TIE2/rtTA/Enb* control mice ( $n = 25$ ), and noninduced *TIE2/rtTA/Enb-TRE/ASTBDN-1* mice ( $n = 6$ ) did not show Tbdn-1 suppression or any ocular disease (Figs. 2c-e, 2g, 4a, 4c, 4e, 5a, 5b, 7d).

The retinal disease in Dox-induced *TIE2/rtTA/Enb-TRE/ASTBDN-1* mice increased in severity with prolonged suppression of Tbdn-1 expression in endothelium (Fig. 6), whereas control mice did not show retinal disease with prolonged Dox induction. *TIE2/rtTA/Enb-TRE/ASTBDN-1* mice fed Dox for 2 weeks showed thickening of the retina and the beginning of the formation of a preretinal membrane harboring neovascular elements in focal areas of the retina (Figs. 6a, 6b). Six weeks after suppression of Tbdn-1 in endothelium, the retinal fibrovascular lesions increased in size (Figs. 6c, 6d). At 6 weeks, retina-lens adhesions, lens-retina fusions, and penetration of aberrant blood vessels through the lens capsule into the lens were evident in some specimens (Figs. 5e, 5f). At a period of 10 to 12 weeks of Tbdn-1 suppression, the fibrovascular lesions of the retina often filled the vitreal space and adhered to the lens (Figs. 5d, 6e, 6f).

### Morphology of Tbdn-1-Suppressed Retinal Lesions

To further characterize the fibrovascular lesions associated with endothelial knockdown of Tbdn-1, we analyzed expression patterns of ECM components by immunohistochemistry in Dox-induced *TIE2/rtTA/Enb-TRE/ASTBDN-1* mice. Laminin expression was used as a marker to label the abnormal retinal

vascular network in Dox-induced *TIE2/rtTA/Enb-TRE/ASTBDN-1* mice and in blood vessels of control retinas (Fig. 4). Sections adjacent to those stained for laminin were analyzed for expression of basement membrane HSPG by using two different anti-basement membrane HSPG monoclonal antibodies (C17 and -33). Results using both anti-HSPG antibodies revealed that expression levels of basement membrane HSPG in blood vessels of retinal lesions resulting from Tbdn-1 suppression were very low or undetected compared with normal retinal blood vessels expressing normal levels of Tbdn-1 (results using antibody C17 shown in Figs. 4c, 4d). Moreover, knockdown of Tbdn-1 expression in endothelium also resulted in a global decrease in retinal basement membrane HSPG expression, including retinal blood vessels localized outside the fibrovascular lesions in areas where the retina appeared normal (Fig. 4e, 4f).

To characterize further the type of cells present in the retinal lesions of Tbdn-1-suppressed animals, retinas of Dox-induced *TIE2/rtTA/Enb-TRE/ASTBDN-1* mice were analyzed for expression of  $\alpha$ -SMA, a myofibroblast cell marker, and GFAP, a glial cell marker. Expression of  $\alpha$ -SMA was detected in the fibrovascular lesions of Dox-induced *TIE2/rtTA/Enb-TRE/ASTBDN-1* mice (Fig. 7a).  $\alpha$ -SMA immunostaining in the retinal lesions appeared to be concentrated around larger blood vessels in a continuous pattern, rather than in a discontinuous one

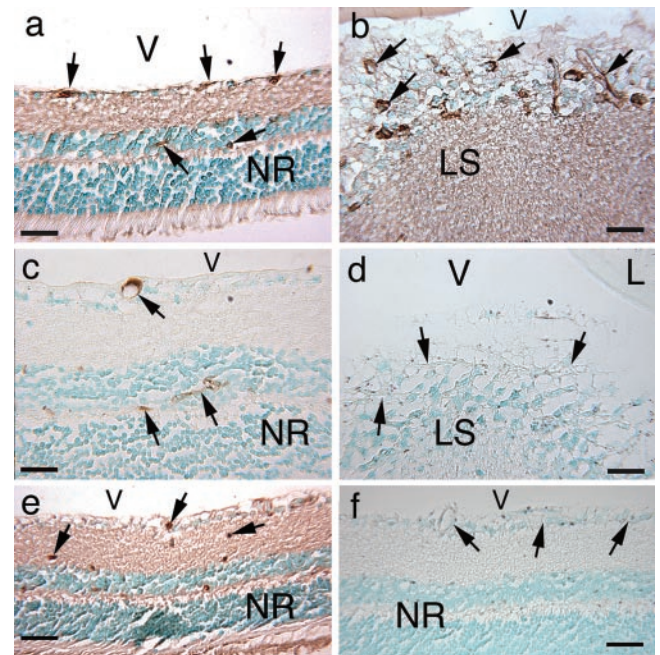


**FIGURE 4.** Endothelial knockdown of Tbdn-1 resulted in suppression of HSPG expression in retinal blood vessels. (a, b) Laminin staining (brown, horseradish peroxidase) labeled the basal lamina of vessels (arrows) revealing the vascular networks present in the retina of both noninduced control (a) and 6-week Dox-induced *TIE2/rtTA/Enb-TRE/ASTBDN-1* mice (b). Laminin expression patterns revealed an increase in retinal blood vessels in Dox-induced *TIE2/rtTA/Enb-TRE/ASTBDN-1* mice showing suppressed Tbdn-1 levels (b). (c, d) In contrast to normal vessels in noninduced *TIE2/rtTA/Enb-TRE/ASTBDN-1* retina (c), vessels (d, arrows) present in the retinal fibrovascular lesions of Tbdn-1-suppressed mice (6-week Dox-induced *TIE2/rtTA/Enb-TRE/ASTBDN-1*) showed low or no brown staining for HSPG. (e, f) Ocular vessels outside fibrovascular lesions (arrows) in Dox-induced *TIE2/rtTA/Enb-TRE/ASTBDN-1* mice also showed normal levels of laminin staining (e) but suppressed levels of HSPG (f) compared with control mice expressing normal levels of Tbdn-1 (a, c, respectively). Counterstain of all sections was methyl green. V, vitreous; NR, neural retina; L, lens; LS, retinal lesion. Scale bars, 25  $\mu$ m. Magnification,  $\times 250$ .

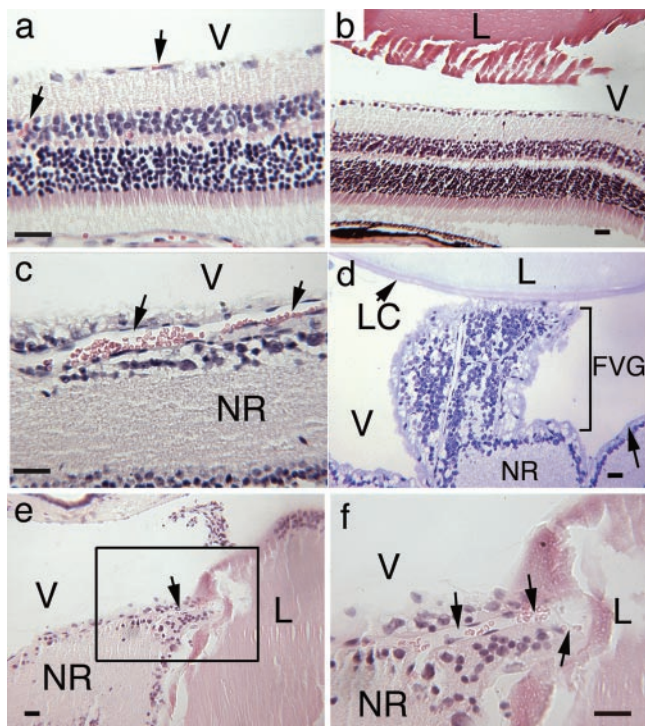


**FIGURE 5.** Endothelial suppression of *Tbdn-1* expression results in retinal neovascularization, preretinal fibrovascular lesions and retina-lens adhesions. Control 6-week Dox-induced *TRE/ASTBDN-1* transgenic (a) and noninduced *TIE2/rtTA/Enb-TRE/ASTBDN-1* bitransgenic (b) retinas did not show any disease. (a, arrows) Normal retinal blood vessels in a control retina. (c) In striking contrast, Dox-induced (12-week) *TIE2/rtTA/Enb-TRE/ASTBDN-1* mice presented large, abnormal, distended vessels extending along the retina (arrows). (d) Dox-induced (10-week) *TIE2/rtTA/Enb-TRE/ASTBDN-1* retinas also exhibited fibrovascular growth extending from the ILM (arrow, bottom right) and adhering to the lens capsule. (e, f) *Tbdn-1*-suppressed retinal vessels (arrows) from Dox-induced (6-week) mice also invaded through the lens capsule. (f) Magnified view of the boxed area in (e) showing the blood vessel (arrows) invading through the lens capsule and extending into the lens. (a–c, e, f) H & E staining; (d) toluidine blue staining. L, lens; LC, lens capsule; V, vitreous; NR, neural retina; FVG, fibrovascular growth. Scale bars, 25  $\mu$ m. Magnification: (a, c, e)  $\times 250$ ; (b, d, e)  $\times 100$ .

that would indicate the normal pericytic coverage of capillaries.  $\alpha$ -SMA staining outside the retinal lesions in *Tbdn-1*-suppressed animals displayed an expression pattern similar to control retinas (Fig. 7c and not shown). Fibrovascular retinal lesions resulting from *Tbdn-1* suppression also show an increase in the number of cells positive for GFAP staining compared with control retinas expressing normal levels of *Tbdn-1* (Figs. 7b, 7d). However, the increase in the number of GFAP-positive cells in *Tbdn-1*-suppressed retinas was restricted to the fibrovascular lesions (data not shown).

#### Location of Disease Associated with the Endothelial Knockdown of *Tbdn-1*

Although retinal lesions in *Tbdn-1*-suppressed mice showed neovascularization with highly abnormal blood vessels and fibrovascular proliferation (Figs. 2, 4, 5, 6, 7), we next quantified the tissue morphometrics to understand better the relationship between retinal and choroidal blood vessel density and changes in tissue thickness resulting from the fibrovascular proliferation. Blood vessel densities in the inner retinal layers including inner limiting membrane (ILM), ganglion cell layer (GCL), inner plexiform layer (IPL), and inner nuclear layer

(INL) were not significantly different in *Tbdn-1*-suppressed retinas compared with control specimens (Fig. 8a). However, the outer plexiform layer in *Tbdn-1*-suppressed retinas showed a significant increase in blood vessel density compared with control animals after 2 weeks of Dox induction but not after 6 or 12 weeks (Fig. 8a). Tissue thicknesses in both the inner and outer retinal layers were significantly increased with length of time of Dox induction from 2 to 12 weeks in *Tbdn-1*-suppressed retinas compared with control specimens (Fig. 8b). Blood vessel densities in the choroid of *Tbdn-1*-suppressed mice were significantly increased (1.8-fold) at 2 weeks of Dox induction compared with control specimens (Fig. 8c). By 12 weeks of Dox induction, the tissue thickness of the choroid was significantly increased in *Tbdn-1*-suppressed retinas compared with control specimens (Fig. 8c). The increased blood vessel density in the outer retina and choroid at 2 weeks of Dox induction was confined to areas associated with retinal lesions of *Tbdn-1*-suppressed mice. These results indicate that blood vessel density increases significantly in the outer plexiform and choroid regions soon after endothelial suppression of *Tbdn-1* (2 weeks), whereas tissue thickness of the retina and choroid increases mostly with length of time of *Tbdn-1* suppression.

Because the *TIE2* panendothelial promoter was used for targeting expression of antisense *TBDN-1* exclusively to all endothelial cells, it is conceivable that the vasculature of tissues other than the retina might be susceptible to the potentially deleterious effects of *Tbdn-1* suppression. To investigate, we analyzed several adult tissues of Dox-induced *TIE2/rtTA/Enb-TRE/ASTBDN-1* mice in comparison with control animals

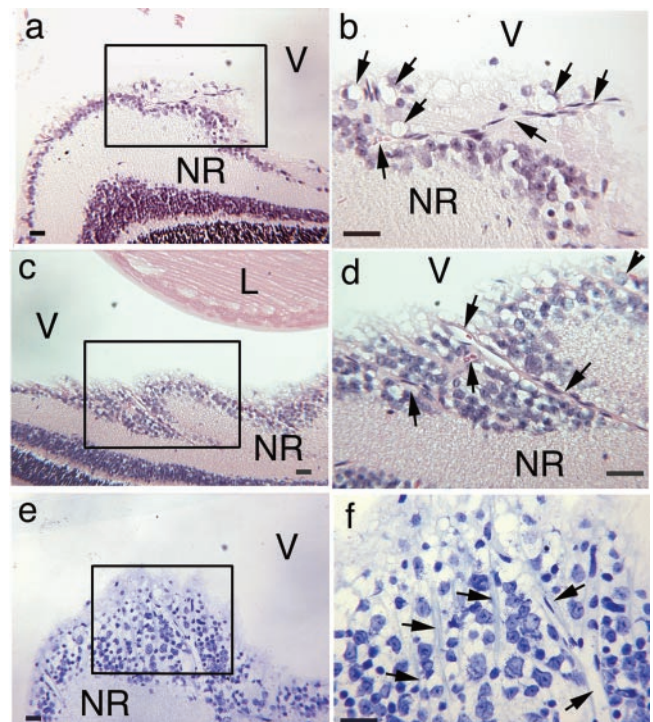


**FIGURE 6.** Retinal lesions increased in severity with prolonged *Tbdn-1* suppression. Retinas from *TIE2/rtTA/Enb-TRE/ASTBDN-1* mice after 2 weeks of Dox induction (a, b) showed evidence of nascent blood vessels and fibrovascular proliferation. The severity of the retinal lesions increased with Dox induction of 6 weeks (c, d) and 10 weeks (e, f). (d, arrows) Neovascularization occurring within the fibrovascular lesions. The boxes in (a) (c), and (e) indicate areas of disease, shown at higher magnification in (b), (d), and (f), respectively. (a–d) H&E staining; (e, f) toluidine blue staining. L, lens; V, vitreous; NR, neural retina. Scale bars, 25  $\mu$ m. Magnification: (a, c, e)  $\times 100$ ; (b, d, f)  $\times 250$ .

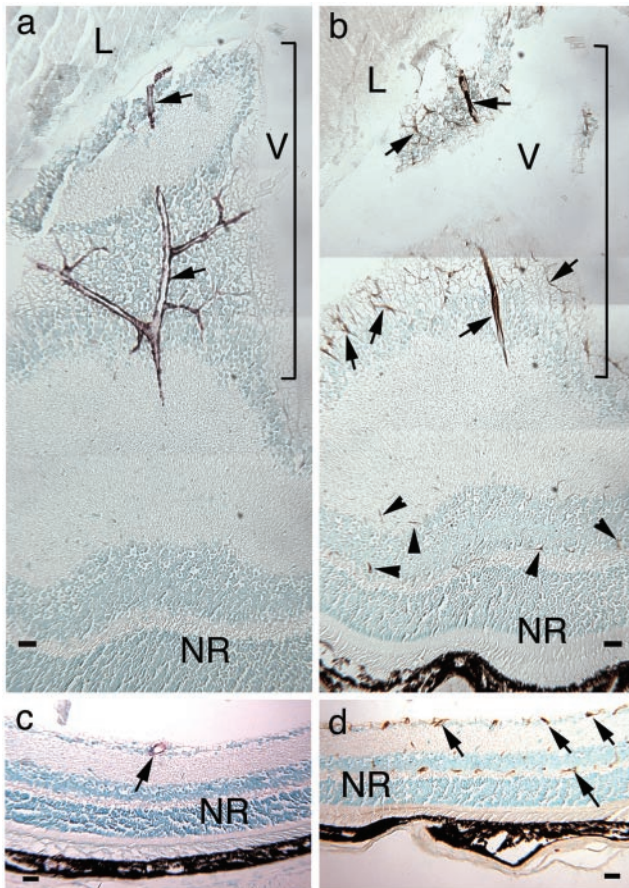


**FIGURE 7.** Fibrovascular lesions in Tbdn-1-suppressed retinas contain myofibroblasts and glial cells. (a)  $\alpha$ -SMA immunostaining (reddish brown, arrows) of a fibrovascular retinal lesion from a 6-week Dox-induced *TIE2/rtTA/Enb-TRE/ASTBDN-1* mouse revealed large abnormal vessels containing myofibroblast cells (bracket), whereas (c) immunostaining outside the lesion displayed a normal pattern. (b) GFAP immunohistochemistry (brown horseradish peroxidase staining) of retinas of 6-week Dox-induced *TIE2/rtTA/Enb-TRE/ASTBDN-1* mice revealed an increase in the number of glial cells (arrows) in fibrovascular tissue (bracket) of retinal lesions compared with (d) control retina expressing normal levels of Tbdn-1. Counterstain of both sections was methyl green. V, vitreous; NR, neural retina; L, lens. Scale bars, 25  $\mu$ m. Magnification,  $\times 100$ .

for disease and for blood vessel integrity, by using endothelial cell and blood vessel markers. Kidney, bone marrow, heart, salivary gland, lung, spleen, liver, brain, and testes from Dox-induced *TIE2/rtTA/Enb-TRE/ASTBDN-1* mice all showed no difference in overall blood vessel density compared with control animals. Figure 8d shows representative blood vessel density in the kidney cortex. Furthermore, areas along surfaces of brain ventricles, (which most closely approximate the anatomy of inner retinal layers) of Dox-induced *TIE2/rtTA/Enb-TRE/ASTBDN-1* mice showed no difference in blood vessel density in comparison with control animals (not shown). Therefore, the neovascularization as well as the pathologic changes evident in Dox-induced *TIE2/rtTA/Enb-TRE/ASTBDN-1* mice appear to be specific to the retina and choroid.

## DISCUSSION

The suppression of Tbdn-1 expression in mouse endothelium resulted in several pathologic features observed in human proliferative retinopathies including retinal neovascularization,

preretinal fibrovascular proliferation, and retina-lens adhesions. Manipulation of specific protein expression has been demonstrated to induce retinal neovascularization in vivo. Previously described models of neovascular retinopathy include overexpression of growth factors. Transgenic mouse models of VEGF overexpression in the retina have been sufficient to cause retinal neovascularization and tractional retinal detachment.<sup>23,24</sup> Transgenic mice overexpressing PDGF-B in photoreceptors soon after birth undergo development of retinal lesions harboring glial, endothelial, and pericyte elements, leading to retinal detachment.<sup>25</sup> However, in contrast to Tbdn-1, the effects of endothelial ablation of PDGF-B are not restricted to the ocular vascular bed,<sup>26</sup> whereas VEGF, an endothelium-specific growth factor, can affect the vasculature of most tissues.<sup>27-29</sup> In the adult, high levels of Tbdn-1 expression are restricted to specialized vasculature, including ocular blood vessels, bone marrow capillaries, atrial endocardium, and blood vessels of regressing ovarian follicles.<sup>16,17</sup> The restriction of pathologic changes to the retina and choroid in Dox-induced *TIE2/rtTA/Enb-TRE/ASTBDN-1* mice indicates that the effects resulting from Tbdn-1 suppression in endothelia is highly specific to retinal and choroidal blood vessels. The lack of disease in other adult tissues might be explained either by the absence of Tbdn-1 expression in the corresponding vascular bed,<sup>16,17</sup> by the absence of a critical binding partner or cofactor important for mediating Tbdn-1 activity in the given tissue, or by presence of a Tbdn-1 homologue that may act in a compensatory manner during Tbdn-1 suppression. Such possible binding partners may include mammalian orthologues of the yeast ARD1 acetyltransferase.<sup>30,31</sup> The Tbdn-1 homologue NAT1 protein, which is expressed in mammalian brain tissue and may play a role in regulating neural responses to cell signaling through the *N*-methyl-D-aspartate pathway,<sup>30</sup> may function in a redundant manner in brain in the absence of Tbdn-1.

Recent published work of others and results presented herein indicate two possible mechanisms that may link decreases in Tbdn-1 expression levels with aberrant retinal blood vessel proliferation. The first possible mechanism of action by which suppression of the Tbdn-1 pathway may lead to retinal blood vessel proliferation may include affecting the stability and/or activity of proteins involved in regulating angiogenesis through acetylation. The acetyltransferase ARD1, which binds the Tbdn-1 homologue of NAT-1, plays a role in the targeted degradation of HIF-1 $\alpha$  in mammals.<sup>32</sup> HIF-1 $\alpha$  regulates VEGF expression during hypoxia and can promote blood vessel proliferation through its induction of VEGF.<sup>33</sup> Suppression or absence of one or more of the acetyltransferase complex-binding partners may disrupt and alter activity of the complex. The disruption of acetyltransferase complexes involving ARD1 or Tbdn-1 may promote the stabilization of HIF-1 $\alpha$  and the production of cytokines promoting neovascularization in the retina.

The second possible mechanism of action by which suppression of the Tbdn-1 pathway may regulate retinal blood vessel proliferation may include deregulation of the expression of HSPG in retinal blood vessels. Our results suggest that Tbdn-1 is an upstream regulator of HSPG expression in blood vessel basement membranes of the retina, since suppression of Tbdn-1 expression leads to loss of HSPG from retinal blood vessel basement membranes. Thickening and alteration of the vascular basement membrane are well-known features associated with proliferative retinopathies.<sup>12,34</sup> Basement membrane ECM constituents provide a tissue-specific barrier between endothelial cells and underlying connective tissues and participate in controlling angiogenesis.<sup>35</sup> Altered expression patterns of ECM constituents could promote the disorganization and breakdown of vascular basement membranes and eventually

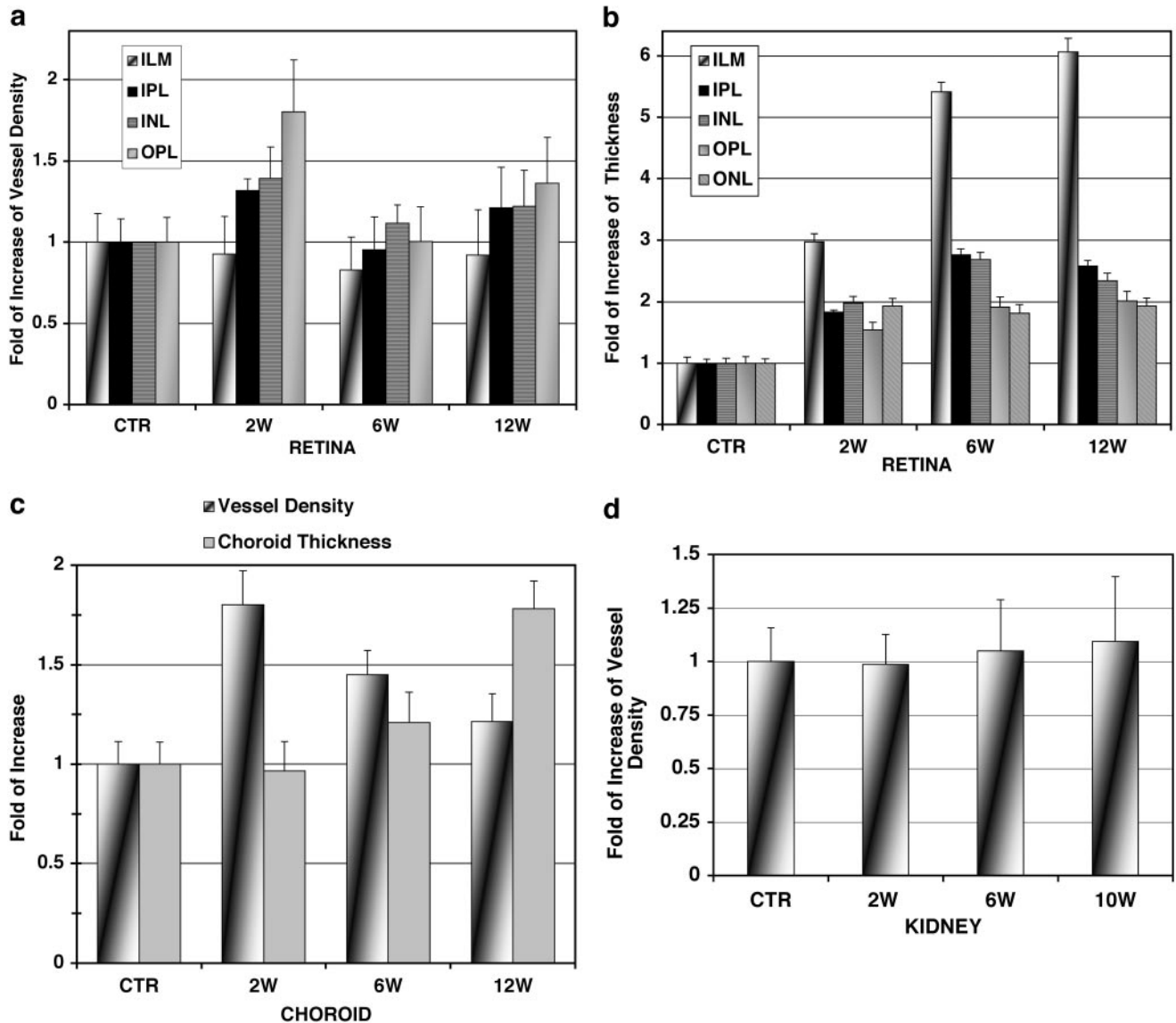


**FIGURE 8.** Morphometric analysis of tissues of Tbdn-1-suppressed mice. Analysis of blood vessel densities (number of blood vessels per square micrometer) of the retinal layers (a), choroid (c), and kidney cortex (d) of Dox-induced *TIE2/rtTA/Enb-TRE/ASTBDN-1* mice after 2, 6, 10, and 12 weeks (W) of suppression of Tbdn-1 expression, compared with control animals (CTR). Control animals include noninduced or Dox-induced wild-type, *TIE2/rtTA/Enb-TRE/ASTBDN-1* mice and noninduced *TIE2/rtTA/Enb-TRE/ASTBDN-1* mice. Dox-induced *TIE2/rtTA/Enb-TRE/ASTBDN-1* mice showed a 1.8-fold increase in outer retinal and choroidal blood vessel density after 2 weeks of Tbdn-1 suppression ( $P < 0.03$ ). A slight but significant increase in choroidal blood vessel density (1.45-fold) was also observed in 6-week Tbdn-1-suppressed mice (c, 6W) ( $P = 0.03$ ). All other time points of Tbdn-1 suppression in the different tissues (retina, choroid, and kidney) did not show significant changes in vessel density. Significant increases in thickness of all retinal layers (b) at all time points of Tbdn-1 suppression (2, 6, and 12 weeks) and at 12 weeks of Tbdn-1 suppression in the choroid (c) were observed ( $P < 0.0003$ ). ILM includes ILM and GCL. Data represent average measurements compared with control  $\pm$  SE.

lead to endothelial cell proliferation.<sup>35</sup> The loss of HSPG from basement membranes has been implicated in the breakdown of blood vessel integrity in diabetic nephropathy.<sup>36–38</sup> Moreover, retinas of diabetic rats show a decrease in the synthesis and expression of the HSPG perlecan.<sup>39</sup> Knockout models of the perlecan gene have been generated but are not informative for evaluating perlecan's role in retinal neovascularization, since the perlecan-null phenotype results in pre- or perinatal lethality.<sup>40</sup> Analysis of the functional importance of blood vessel basement-membrane-specific HSPG such as perlecan must await conditional gene targeting studies that would allow an evaluation of the specific role HSPGs may play in retinal blood vessels. HSPG can regulate the activity of angiogenic factors (e.g., VEGF, bFGF) by regulating the binding to their respective receptor on endothelial cells.<sup>41,42</sup> Currently, it is not clear

whether suppression of basement membrane HSPG in retinal blood vessels of Tbdn-1-suppressed mice is the result of a reduction in HSPG synthesis or an increase in HSPG degradation. Future studies will focus on the identification of specific basement membrane HSPGs regulated by Tbdn-1 and the mechanisms of action underlying this process.

Although retinal detachment is common in later stage PDR, in rodents, retinal detachment is rare.<sup>43</sup> Nevertheless, the retinal disease in Dox-induced *TIE2/rtTA/Enb-TRE/ASTBDN-1* mice displayed several features that could promote tractional retinal detachment. The Tbdn-1-suppressed retinas showed retina-lens adhesions and invasion of the lens capsule and lens by blood vessels from the adjacent fibrovascular lesion tissue. The fibrovascular lesions in Tbdn-1-suppressed retinas showed an increase in the numbers of cells expressing the glial marker

GFAP compared with control retinas. In conjunction with an increase in GFAP-positive cells, the myofibroblastic marker  $\alpha$ -SMA is increased in large-caliber blood vessels in the retinal lesions. Myofibroblasts expressing  $\alpha$ -SMA and glial cells expressing GFAP are thought to be involved in the formation of retinal lesions possessing contractile forces that promote retinal detachment in retinopathy.<sup>44-50</sup> The presence of  $\alpha$ -SMA in larger caliber blood vessels in GFAP positive lesions supports the view that the exertion of contractile force and subsequent tractional retinal detachment is possible in the advanced retinal lesions of Tbdn-1-suppressed mice. The retinal disease in Dox-induced *TIE2/rtTA/Enb-TRE/ASTBDN-1* mice is accompanied by a progressive increase in retinal and choroidal tissue thickness that is reminiscent of the pronounced retinal thickening occurring in proliferative diabetic retinopathy and macular edema in humans<sup>1,2,5,13,17</sup> (reviewed in Refs. 51, 52). The significant retinal tissue thickening (and thus increased tissue volume) in inner retinal layers and choroids of Dox-induced *TIE2/rtTA/Enb-TRE/ASTBDN-1* mice is probably the reason that retinal blood vessel density in the ILM, GCL, IPL, and INL does not change significantly from control with length of time of Tbdn-1 suppression, despite the obvious histopathological changes in the blood vessels feeding these areas of retinal disease (Figs. 2, 4, 5 6, 7). Despite the remodeling of the retinal tissue in Dox-induced *TIE2/rtTA/Enb-TRE/ASTBDN-1* mice to increase retinal tissue volume effectively, we still detected significant increases in blood vessel density in deeper retinal tissue (outer plexiform layer [OPL]) and in the choroid. These results indicate that the Tbdn-1-suppressed mice also have subretinal neovascularization. Subretinal neovascularization is a rare occurrence in genetic mouse models of retinal disease, has been associated only with two mouse models thought to replicate disease occurring in human age-related macular degeneration.<sup>53,54</sup> The disease we report in the current study in deeper retinal layers and choroid in *TIE2/rtTA/Enb-TRE/ASTBDN-1* mice suggests that Tbdn-1-suppressed mice may also be useful for modeling the subretinal neovascularization in human age-related macular degeneration.

The conditional knockdown of Tbdn-1 in endothelium in the *TIE2/rtTA/Enb-TRE/ASTBDN-1* bitransgenic model clearly provides evidence of the necessity of Tbdn-1 expression for the maintenance of adult retinal and choroidal blood vessel homeostasis by suppressing abnormal blood vessel growth. The phenotype associated with Tbdn-1 suppression in endothelium resembles the sight-disrupting disease observed in human proliferative retinopathy. This, together with our previous evidence of Tbdn-1 suppression in the retinal endothelium in patients with PDR,<sup>17</sup> supports the hypothesis of a contributing role of the loss of Tbdn-1 expression in the progression of proliferative retinopathies. Tbdn-1 may serve as a valuable pathway for developing new therapies aimed at controlling proliferative retinopathies.

### Acknowledgments

The authors thank Thomas N. Sato (University of Texas Southwestern) for providing the *TIE2* promoter construct and Lisa Adams and Erin Woodward for expert technical assistance.

### References

- Kohner EM. Diabetic Retinopathy. *BMJ*. 1993;307:1195-1199.
- Infeld DA, O'Shea JG. Diabetic retinopathy. *Postgrad Med J*. 1998;74:129-133.
- Aiello LM. Perspectives on diabetic retinopathy. *Am J Ophthalmol*. 2003;36:122-135.
- Good WV, Gendron RL. Gene therapy for retinopathy of prematurity: the eye is a window to the future. *Br J Ophthalmol*. 2001;85:891-892.
- Paques M, Massin P, Gaudric A. Growth factors and diabetic retinopathy. *Diabetes Metab*. 1997;23:125-130.
- Good WV, Gendron RL. Retinopathy of prematurity. *North Am Clin Ophthalmol*. 2001;14:513-519.
- Early Treatment of Retinopathy of Prematurity Cooperative Group. Revised indications for the treatment of retinopathy of prematurity. *Arch Ophthalmol*. 2003;14:1684-1696.
- Cryotherapy for Retinopathy of Prematurity Cooperative Group. Multicenter trial of cryotherapy for retinopathy of prematurity: ophthalmological outcomes at 10 years. *Arch Ophthalmol*. 2001;119:1110-1118.
- Campochiaro PA, Hackett SF. Ocular neovascularization: a valuable model system. *Oncogene*. 2003;22:6537-6548.
- Miller JW. Vascular endothelial growth factor and ocular neovascularization. *Am J Pathol*. 1997;151:13-23.
- Robinson GS, Aiello LP. Angiogenic factors in diabetic ocular disease: mechanisms of today, therapies for tomorrow. *Int Ophthalmol Clin*. 1998;38:89-102.
- Ljubimov AV, Burgeson RE, Butkowsky RJ, et al. Basement membrane abnormalities in human eyes with diabetic retinopathy. *J Histochem Cytochem*. 1996;44:1469-1479.
- Hosoda Y, Okada M, Matsumura M, et al. Epiretinal membrane of proliferative diabetic retinopathy: an immunohistochemical study. *Ophthalmic Res*. 1993;25:289-294.
- Hammes HP, Lin J, Bretze RG, Brownlee M, Breier G. Upregulation of the vascular endothelial growth factor/vascular endothelial growth factor receptor system in experimental background diabetic retinopathy of the rat. *Diabetes*. 1998;47:401-406.
- Amin RH, Frank RN, Kennedy A, Elliott D, Puklin JE, Abrams GW. Vascular endothelial growth factor is present in glial cells of the retina and optic nerve of human subjects with nonproliferative diabetic retinopathy. *Invest Ophthalmol Vis Sci*. 1997;38:36-47.
- Gendron RL, Adams LC, Paradis H. Tubedown-1, a novel acetyltransferase associated with blood vessel development. *Dev Dyn*. 2000;218:300-315.
- Gendron RL, Good WV, Adams LC, Paradis H. Expression of tubedown-1 is suppressed in retinal neovascularization of proliferative diabetic retinopathy. *Invest Ophthalmol Vis Sci*. 2001;42:3000-3007.
- Paradis H, Liu CY, Saika S, et al. Tubedown-1 in TGF- $\beta$ 2 mediated remodeling of the developing vitreal vasculature in vivo and regulation of capillary outgrowth in vitro. *Dev Biol*. 2002;249:140-155.
- Schlaeger TM, Bartunkova S, Lawitts JA, et al. Uniform vascular-endothelial-cell-specific gene expression in both embryonic and adult transgenic mice. *Proc Natl Acad Sci USA*. 1997;94:3058-3063.
- Gendron RL, Tsai F-Y, Paradis H, Arcenci RJ. Induction of embryonic vasculogenesis by bFGF and LIF in vitro and in vivo. *Dev Biol*. 1996;177:332-347.
- Sanes JR, Chiu AY. The basal lamina of the neuromuscular junction. *Cold Spring Harbor Symp Quant Biol*. 1983;48:667-678.
- Bayne EK, Anderson MJ, Fambrough DM. Extracellular matrix organization in developing muscle: correlation with acetylcholine receptor aggregates. *J Cell Biol*. 1984;99:1486-1501.
- Tobe T, Okamoto N, Viores MA, et al. Evolution of neovascularization in mice with overexpression of vascular endothelial growth factor in photoreceptors. *Invest Ophthalmol Vis Sci*. 1998;39:180-188.
- Ozaki H, Seo MS, Ozaki K, et al. Blockade of vascular endothelial cell growth factor receptor signaling is sufficient to completely prevent retinal neovascularization. *Am J Pathol*. 2000;156:697-707.
- Viores SA, Seo MS, Derevanik NL, Campochiaro PA. Photoreceptor-specific overexpression of platelet-derived growth factor induces proliferation of endothelial cells, pericytes, and glial cells and aberrant vascular development: an ultrastructural and immunocytochemical study. *Brain Res Dev Brain Res*. 2003;140:169-183.
- Engel M, Bjarnegard M, Gerhardt H, et al. Endothelium-specific platelet-derived growth factor-B ablation mimics diabetic retinopathy. *EMBO J*. 2002;21:4307-4316.

27. Dor Y, Djonov V, Keshet E. Induction of vascular networks in adult organs: implications to proangiogenic therapy. *Ann NY Acad Sci.* 2003;995:208–216.
28. Dor Y, Djonov V, Keshet E. Making vascular networks in the adult: branching morphogenesis without a roadmap. *Trends Cell Biol.* 2003;13:131–136.
29. Dor Y, Djonov V, Abramovitch RI, et al. Conditional switching of VEGF provides new insights into adult neovascularization and pro-angiogenic therapy. *EMBO J.* 2002;21:1939–1947.
30. Sugiura N, Adams SM, Corriveau RA. An evolutionarily conserved N-terminal acetyltransferase complex associated with neuronal development. *J Biol Chem.* 2003;278:40113–40120.
31. Jeong JW, Bae MK, Ahn MY, et al. Regulation and destabilization of HIF-1alpha by ARD1-mediated acetylation. *Cell.* 2002;111:709–720.
32. Park EC, Szostak JW. ARD1 and NAT1 proteins form a complex that has N-terminal acetyltransferase activity. *EMBO J.* 1992;11:2087–2093.
33. Ozaki H, Yu AY, Della N, et al. Hypoxia inducible factor-1alpha is increased in ischemic retina: temporal and spatial correlation with VEGF expression. *Invest Ophthalmol Vis Sci.* 1999;40:182–189.
34. Tsilibary EC. Microvascular basement membranes in diabetes mellitus. *J Pathol.* 2003;200:537–546.
35. Kalluri R. Basement membranes: structure, assembly, and role in tumor angiogenesis. *Nat Rev.* 2003;3:422–433.
36. Raats CJ, Van Den Born J, Berden JH. Glomerular heparan sulfate alterations: mechanisms and relevance for proteinuria. *Kidney Int.* 2000;57:385–400.
37. Jensen T. Pathogenesis of diabetic vascular disease: evidence for the role of reduced heparan sulfate proteoglycan. *Diabetes.* 1997;46:S98–S100.
38. Conde-Knape K. Heparan sulfate proteoglycans in experimental models of diabetes: a role for perlecan in diabetes complications. *Diabetes Metab Res Rev.* 2001;17:412–421.
39. Bollineni JS, Allura I, Reddi AS. Heparan sulfate proteoglycan synthesis and its expression are decreased in the retina of diabetic rats. *Curr Eye Res.* 1997;16:127–130.
40. Forsberg E, Kjellen L. Heparan sulfate: lessons from knockout mice. *J Clin Invest.* 2001;108:175–180.
41. Fannon M, Forsten-Williams K, Dowd CJ, Freedman DA, Folkman J, Nugent MA. Binding inhibition of angiogenic factors by heparan sulfate proteoglycans in aqueous humor: potential mechanism for maintenance of an avascular environment. *FASEB J.* 2003;17:902–904.
42. Iivanainen E, Kahari VM, Heino J, Elenius K. Endothelial cell-matrix interactions. *Microsc Res Tech.* 2003;60:13–22.
43. Smith RS, Retina. John SWM, Nishina PM, Sundberg JP, eds. *Systematic Evaluation of the Mouse Eye: Anatomy, Pathology, and Biomethods.* Boca Raton, FL: CRC Press; 2002:216.
44. Bochaton-Piallat ML, Kapetanios AD, Donati G, Redard M, Gabbiani G, Pournaras CJ. TGF-beta1, TGF-beta receptor II and ED-A fibronectin expression in myofibroblast of vitreoretinopathy. *Invest Ophthalmol Vis Sci.* 2000;41:2336–2342.
45. Gandorfer A, Rohleder M, Kampik A. Epiretinal pathology of vitreomacular traction syndrome. *Br J Ophthalmol.* 2002;86:902–909.
46. Zhang Y, Stone J. Role of astrocytes in the control of developing retinal vessels. *Invest Ophthalmol Vis Sci.* 1997;38:1653–1666.
47. Li Q, Zemel E, Miller B, Perlman I. Early retinal damage in experimental diabetes: electroretinographical and morphological observations. *Exp Eye Res.* 2002;74:615–625.
48. Rungger-Brandle E, Dosso AA, Leuenberger PM. Glial reactivity, an early feature of diabetic retinopathy. *Invest Ophthalmol Vis Sci.* 2002;41:1971–1980.
49. Sennlaub F, Valamanesh F, Vazquez-Tello A, et al. Cyclooxygenase-2 in human and experimental ischemic proliferative retinopathy. *Circulation.* 2003;108:198–204.
50. Guidry C, Bradley KM, King JL. Tractional force generation by human Müller cells: growth factor responsiveness and integrin receptor involvement. *Invest Ophthalmol Vis Sci.* 2003;44:1355–1363.
51. Speicher MA, Danis RP, Criswell M, Pratt L. Pharmacologic therapy for diabetic retinopathy. *Expert Opin Emerg Drugs.* 2003;8:239–250.
52. Panozzo G, Gusson E, Parolini B, Mercanti A. Role of OCT in the diagnosis and follow up of diabetic macular edema. *Semin Ophthalmol.* 2003;18:74–81.
53. Smith RS, John SW, Zabeleta A, Davisson MT, Hawes NL, Chang B. The bst locus on mouse chromosome 16 is associated with age-related subretinal neovascularization. *Proc Natl Acad Sci USA.* 2000;29:2191–2195.
54. Ambati J, Anand A, Fernandez S, et al. An animal model of age-related macular degeneration in senescent Ccl-2 or Ccn-2-deficient mice. *Nature Med.* 2003;9:1390–1397.